Available online at www.sciencedirect.com
ScienceDirect
International Journal of Thermal Sciences 46 (2007) 213–220
International Journal of Thermal Sciences
www.elsevier.com/locate/ijts

Study of the effect of convection on close contact melting of high Prandtl number substances

Dominic Groulx *, Marcel Lacroix

Département de génie mécanique, Université de Sherbrooke, Sherbrooke (Québec), Canada J1K 2R1

Received 19 January 2006; received in revised form 13 April 2006; accepted 14 April 2006

Available online 9 August 2006

Abstract

A study is conducted to examine the role of convection on close contact melting of a high Prandtl number phase change material, i.e. ice, resting on a heated plate. A convection dominated model is proposed and its predictions are compared to a conduction dominated model and to experimental data. Results indicate that convection plays a leading role in the process of close contact melting for $Ste_{\text{eff}} \geqslant 0.1$. Convection reduces the heat flux at the solid–liquid interface thereby slowing down the melting rate. The effect of inertia forces is negligible during the entire melting process while surface tension becomes important only near the end. It is also shown that buoyancy forces reduce the heat transfer rate at the solid–liquid interface.

Sommaire

Le rôle de la convection lors de la fusion par contact direct de substances au nombre de Prantl grand, comme la glace, est examine. Un modèle mathématique de convection est présenté et ses predictions sont comparées à celles d'un modèle de conduction et à des mesures expérimentales. Les résultats montrent que la convection deviant incontournable pour $Ste_{\text{eff}} \geqslant 0.1$. La convection réduit le flux de chaleur à l'interface solide–liquide et par conséquent ralentit le processus de fusion. L'effet des forces d'inertie est négligeable pendant toute la durée de la fusion alors que l'effet de la tension superficielle devient important vers la fin. On observe également que les forces d'Archimède réduisent le flux de chaleur à l'interface solide–liquide.

Keywords: Contact melting; Convection; Ice; Experiments; Analytical model

Mots-clés : Fusion par contact direct ; Convection ; Glace ; Expériences ; Modèle analytique

1. Introduction

Over the last two decades, solid–liquid phase change heat transfer has received increasing research attention in the open literature [1]. This type of heat transfer finds applications in the melting of ice and the solidification of water [2], the purification of metals [3], the study of geophysical phenomena (fusion of glaciers and volcanic eruptions) [4], the cooling of electronic equipments [5] and the thermal control of space stations and vehicles [6].

Different modes of heat transfer such as conduction, convection, radiation and close contact melting may be involved in a system that undergoes solid–liquid phase change [1]. The mode that is of particular interest to the authors here is close contact melting. Close contact melting occurs when a solid melts while being in contact with a heat source. The liquid generated at the melting front is squeezed out from under the solid by the pressure maintained in the central section of the film by the weight of the free solid.

The problem of close contact melting has been the subject of a number of investigations related to the fundamentals of heat transfer [4,7–11], lubrication [1] and latent heat energy storage [12–14]. Close contact melting is primarily studied because the heat fluxes across the melt layer separating the heat surface

* Corresponding author.
E-mail address: d.groulx@USherbrooke.ca (D. Groulx).

1290-0729/$ – see front matter
doi:10.1016/j.ijthermalsci.2006.04.017

Nomenclature

Dimensional variables

C	heat capacity	$\mathrm{J\,kg^{-1}\,K^{-1}}$
F	forces, other than pressure	N
g	acceleration of gravity	$\mathrm{m\,s^{-2}}$
h	latent heat of fusion	$\mathrm{J\,kg^{-1}}$
H	initial height of the block	m
k	thermal conductivity	$\mathrm{W\,m^{-1}\,K^{-1}}$
L	length of the block	m
P	pressure	Pa
Q	flow rates	$\mathrm{m^2\,s^{-1}}$
S	molten height of the block	m
t	time	s
T	temperature	K
u	x velocity component	$\mathrm{m\,s^{-1}}$
v	y velocity component	$\mathrm{m\,s^{-1}}$
w	z velocity component	$\mathrm{m\,s^{-1}}$
U	speed of the liquid in the gap	$\mathrm{m\,s^{-1}}$
V	melting speed	$\mathrm{m\,s^{-1}}$
x	coordinate	m
y	coordinate	m
z	coordinate	m

Greek symbols

α	thermal diffusivity of melt	$\mathrm{m^2\,s^{-1}}$
δ	molten layer thickness	m
ΔT	temperature difference $(T_\mathrm{p} - T_\mathrm{m})$	K
Φ	viscous dissipation	$\mathrm{m^2\,s^{-2}}$
λ	roots of a Laplace equation	
μ	dynamic viscosity	$\mathrm{N\,s\,m^{-2}}$
ν	kinematic viscosity	$\mathrm{m^2\,s^{-1}}$
ρ	density	$\mathrm{kg\,m^{-3}}$
σ	surface tension	$\mathrm{N\,m^{-1}}$

Non-dimensional variables

C_1	function dependent on the geometry
C_2	function dependent on the height of the block and the surface tension
C_Ste	function dependent on the plate temperature
C_σ	function dependent on the surface tension

Subscripts

eff	effective
f	liquid
m	melting point
n	indices of summation
p	plate
s	solid
sc	subcooled
tot	total melt
x	in the x direction
z	in the z direction

Superscripts

$*$	indicates dimensionless quantity

Definitions of non-dimensional variables

Ec	Eckert number $U^2/C\Delta T$
Oh	Ohnesorge number $\mu/\sqrt{\rho L\sigma}$
Nu	Nusselt number $q''/(k_\mathrm{f}\Delta T/L_x)$
Pr	Prandtl number ν/α
Ste	Stefan number $C\Delta T/h_\mathrm{fs}$

from the solid phase change material (PCM) are generally high. As a result, the melting times are considerably reduced compared to that observed for other heat transfer modes.

In most of the previous studies on close contact melting, the process by which the melt is squeezed out of the small gap separating the heat source and the solid was assumed to be quasi-steady and the heat transfer through the liquid film was considered to be conduction dominated [1,4,8–10,12–14]. Recent studies suggest however that this last assumption may, in some cases, no longer be valid as convection heat transfer prevails in the thin melt layer [11,16–18]. For instance, Saito et al. [11] and Yoo et al. [18] have carried out numerical analyses showing that the heat transfer in the liquid film is affected by the effect of convection in the case of *Ste* number larger than 0.1. They suggest that the melting rate decreases at high *Ste* number because the heat capacity of molten liquid increases with *Ste*.

In a previous article [16], the authors showed, by performing an order of magnitude analysis, that convection and inertia forces play a role in the melting process when a relative velocity is imposed between the PCM block and the heated plate regardless of the Prandtl number of the melting substance. For $Re > 0$, it was found that convection enhances the melting process. The present paper further investigates this matter by focusing on the case for which there is no relative motion between the PCM block and the heated surface.

First, a new mathematical model that accounts for the effect of convection is proposed. The objective is to predict accurately the contact melting behaviour of PCMs with a mathematical model simple enough to be used in engineering applications. Next, an experimental rig is erected and experiments are carried out for the melting of a high Prandtl number substance, i.e., ice. The effect of convection heat transfer on close contact melting is then delineated in terms of the *Ste* number. The role of inertia, buoyancy and surface tension on the melting process is also examined.

2. Mathematical model and physical analysis

A schematic representation of the physical system is depicted in Fig. 1. A block of solid PCM of initial height H, length L_x and depth L_z initially at uniform subcooled temperature $T_\mathrm{m} - T_\mathrm{sc}$ rests on a flat plate. At time $t = 0$, the temperature of the flat plate is suddenly raised to a constant value $T_\mathrm{p} = T_\mathrm{m} + \Delta T$. Melting is triggered and the solid descends ver-

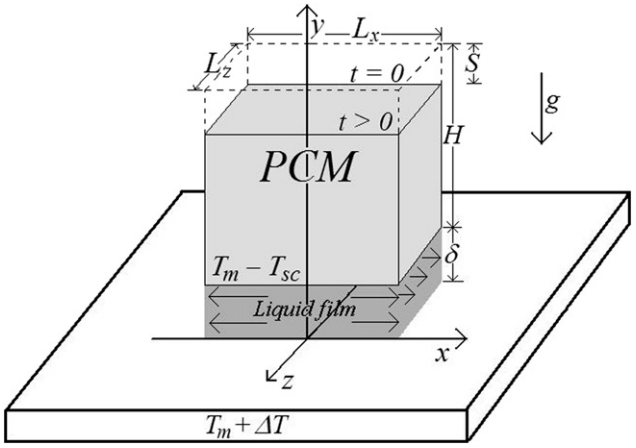

Fig. 1. Schematic of the system.

tically at a speed V while squeezing the melt out of the thin gap of thickness δ between the solid and the plate.

Six assumptions are made regarding the behaviour of the physical system:

(1) The melting process is considered quasi-steady, i.e., at every point in time the weight of the solid is balanced by the excess pressure built in the liquid film (plus any other relevant forces);
(2) The heat transfer is one-dimensional (function of y only) but the dynamic process is two-dimensional (conservation of momentum in two direction, x and z);
(3) The liquid film thickness δ is constant along the length L_x and L_z of the block (this assumption results from 2). δ may, however, vary with time;
(4) The flow in the liquid film remains laminar;
(5) The fluid properties are temperature independent and are evaluated at the film temperature ($T_{\text{film}} = T_{\text{m}} + \Delta T/2$);
(6) The temperature of the PCM block is considered constant throughout the melting process.

2.1. Governing equations

Based on these above assumptions, the general mass, momentum and energy conservation equations for the fluid layer may be stated as:

$$\frac{\partial u}{\partial x} + \frac{\partial v}{\partial y} + \frac{\partial w}{\partial z} = 0 \tag{1}$$

$$u\frac{\partial u}{\partial x} + v\frac{\partial u}{\partial y} + w\frac{\partial u}{\partial z} = \frac{-1}{\rho_{\text{f}}}\frac{\mathrm{d}P}{\mathrm{d}x} + \nu_{\text{f}}\left(\frac{\partial^2 u}{\partial x^2} + \frac{\partial^2 u}{\partial y^2} + \frac{\partial^2 u}{\partial z^2}\right) \tag{2}$$

$$u\frac{\partial w}{\partial x} + v\frac{\partial w}{\partial y} + w\frac{\partial w}{\partial z} = \frac{-1}{\rho_{\text{f}}}\frac{\mathrm{d}P}{\mathrm{d}z} + \nu_{\text{f}}\left(\frac{\partial^2 w}{\partial x^2} + \frac{\partial^2 w}{\partial y^2} + \frac{\partial^2 w}{\partial z^2}\right) \tag{3}$$

$$u\frac{\partial T}{\partial x} + v\frac{\partial T}{\partial y} + w\frac{\partial T}{\partial z} = \alpha_{\text{f}}\left(\frac{\partial^2 T}{\partial x^2} + \frac{\partial^2 T}{\partial y^2} + \frac{\partial^2 T}{\partial z^2}\right) + \frac{\mu_{\text{f}}}{\rho_{\text{f}} C_{\text{f}}}\Phi \tag{4}$$

Furthermore, at the solid–liquid interface ($y = \delta$), an energy balance yields

$$-k_{\text{f}}\left(\frac{\mathrm{d}T}{\mathrm{d}y}\right)_{y=\delta} = \rho_{\text{s}} V (h_{\text{fs}} + C_{\text{s}} T_{\text{sc}}) \tag{5}$$

It is also assumed that at all times the pressure in the liquid gap is related to the weight of the PCM block and to other forces by:

$$\int_{-L_x/2}^{L_x/2}\int_{-L_z/2}^{L_z/2} P(x,z)\,\mathrm{d}x\,\mathrm{d}z + F = \rho_{\text{s}}(H - S)L_x L_z g \tag{6}$$

To simplify the above system of equations, an order of magnitude analysis is performed. To make sense of this analysis, it is instructive to look first at a conduction model which was put forth by Bejan [15].

2.2. Bejan's model

Bejan's model presents a simple and elegant solution for the problem of close contact melting on a heated flat plate. In this model, heat transfer is considered one dimensional, subcooling in the solid phase is ignored and the pressure in the liquid layer is balanced by the weight of the block. The model rests on the following equations (full details on the mathematical model are reported in reference [15]):

$$\frac{\partial u}{\partial x} + \frac{\partial v}{\partial y} = 0 \tag{7}$$

$$\frac{\partial^2 u}{\partial y^2} = \frac{1}{\mu_{\text{f}}}\frac{\mathrm{d}P}{\mathrm{d}x} \tag{8}$$

$$\frac{\partial^2 T}{\partial y^2} = 0 \tag{9}$$

$$-k_{\text{f}}\left(\frac{\mathrm{d}T}{\mathrm{d}y}\right)_{y=\delta} = \rho_{\text{s}} V h_{\text{fs}} \tag{10}$$

$$\int_{-L_x/2}^{L_x/2} P(x)\,\mathrm{d}x = \rho_{\text{s}}(H - S)L_x g \tag{11}$$

In this model, inertia in the momentum equation (Eq. (8)) and viscous dissipation and convection in the energy equation (Eq. (9)) are neglected. However, in a recent study [16] it was shown that inertia is negligible with respect to friction if

$$\frac{V\delta}{\mu_{\text{f}}} \ll 1 \tag{12}$$

which translates into Bejan's solution as:

$$\frac{Ste}{Pr} \ll 1 \tag{13}$$

This condition is satisfied for high Prandtl number substances and/or small Stefan numbers. For low Prandtl number

substances however, i.e., liquid metals, the above condition suggests that inertia forces may no longer be neglected in the melting process. On the other hand, the effect of viscous dissipation can be ignored in comparison to that of conduction if,

$$Pr \cdot Ec \ll 1 \tag{14}$$

The above condition is always satisfied in the case of a fixed heated plate. Finally, the effect of convection is negligibly small with respect to that of conduction if

$$\frac{V\delta}{\alpha_f} \ll 1 \tag{15}$$

Again, in Bejan's model this condition becomes

$$Ste \ll 1 \tag{16}$$

which is independent of the Prandtl number.

Based on these observations, it is expected that convection heat transfer may play an important role in close contact melting for $Ste \geqslant 0.1$. As a result, it cannot be overlooked in the model.

2.3. Proposed model

Bejan's model for close contact melting was improved in order to account for the effect of convection. The revised model rests on the following conservation equations:

$$\frac{\partial u}{\partial x} + \frac{\partial v}{\partial y} + \frac{\partial w}{\partial z} = 0 \tag{1}$$

$$\frac{\partial^2 u}{\partial y^2} = \frac{1}{\mu_f}\frac{dP}{dx} \tag{8}$$

$$\frac{\partial^2 w}{\partial y^2} = \frac{1}{\mu_f}\frac{dP}{dz} \tag{17}$$

$$\frac{\partial^2 T}{\partial y^2} = -\frac{V}{\alpha_f}\frac{\partial T}{\partial y} \tag{18}$$

$$-k_f\left(\frac{dT}{dy}\right)_{y=\delta} = \rho_s V(h_{fs} + C_s T_{sc}) \tag{5}$$

$$\int_{-L_x/2}^{L_x/2}\int_{-L_z/2}^{L_z/2} P(x,z)\,dx\,dz + F = \rho_s(H-S)L_xL_zg \tag{6}$$

where the velocity component v is approximated as the melting speed V at the melting interface ($y = \delta$). The boundary conditions for the momentum equations (8) and (17) are $u(y=0) = 0, u(y=\delta) = 0, w(y=0) = 0$ and $w(y=\delta) = 0$ respectively. The boundary conditions for the temperature equation (18) are $T(y=0) = T_p = T_m + \Delta T$ and $T(y=\delta) = T_m$. The other force (F) in Eq. (6) takes into account the effect of surface tension via the following expression

$$F = 2\sigma_f(L_x + L_z) \tag{19}$$

The temperature distribution in the liquid layer is obtained from the solution of Eq. (18):

$$T(y) = T_m + \Delta T\frac{\{\exp(-Vy/\alpha_f) - \exp(-V\delta/\alpha_f)\}}{1 - \exp(-V\delta/\alpha_f)} \tag{20}$$

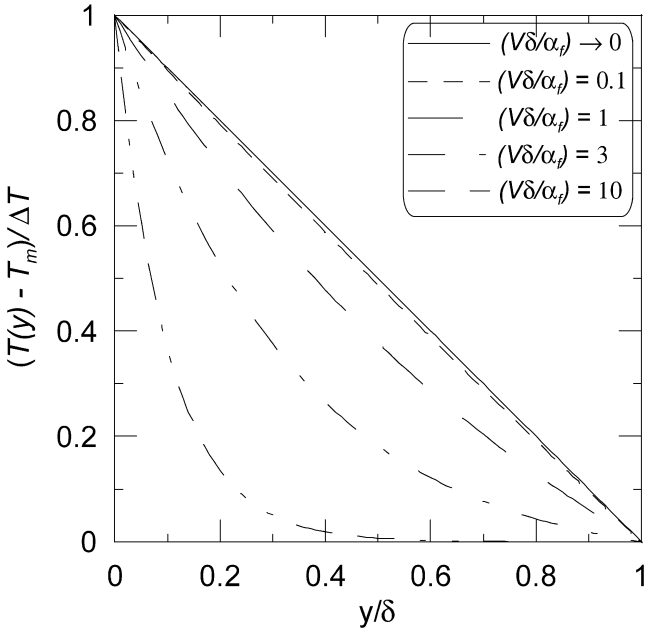

Fig. 2. Temperature profile in the melt layer.

This temperature profile is plotted in Fig. 2. It is seen that the effect of convection becomes increasingly important for $(V\delta/\alpha_f) > 0.1$. For these cases, the linear temperature profile assumed in Bejan's model is no longer valid. Indeed, as the dimensionless parameter $V\delta/\alpha_f$ increases in magnitude, the mean temperature of the liquid in the melt gap gets closer to the melting point T_m and, as a result, the heat flux at the melting front diminishes and so the melting rate.

Substitution of Eq. (20) into Eq. (5) provides a first relation between the molten layer thickness δ and the melting speed V:

$$-\rho_f C_f\frac{\Delta T}{1 - \exp(V\delta/\alpha_f)} = \rho_s(h_{fs} + C_s T_{sc}) \tag{21}$$

The velocity profile for u is found from the solution of Eq. (8), i.e.,

$$u(y) = \frac{1}{2\mu_f}\frac{\partial P}{\partial x}y(y-\delta) \tag{22}$$

This solution cannot be used yet because it involves the unknown pressure gradient $\partial P/\partial x$. The pressure must be related to the normal force with which the melting block is pushed downward. The pressure distribution is determined first by calculating the liquid flow rate

$$Q_x(x) = \int_0^\delta u(x,y)\,dy \tag{23}$$

Then, integration of the continuity equation (Eq. (1)) from $y = 0$ ($v = 0$) to $y = \delta$ ($v = -V$) yields,

$$\frac{dQ_x(x)}{dx} + \frac{dQ_z(z)}{dz} = V \tag{24}$$

Substituting Eqs. (22) and (23) into (24), the following differential relation between the pressure P, the melting speed V, and the liquid film height δ is obtained:

$$\frac{\partial^2 P}{\partial x^2} + \frac{\partial^2 P}{\partial z^2} = -\frac{12\mu_f V}{\delta^3} \tag{25}$$

Using the boundary conditions for the pressure $P(x = \pm L_x/2) = 0$ and $P(z = \pm L_z/2) = 0$, the solution for the Poisson equation (25) is:

$$P(x,z) = \frac{3}{2}\frac{\mu_f V}{\delta^3}\left[\left(L_x^2 - 4x^2\right) + \frac{32}{L_x}\sum_{n=0}^{\infty}\frac{(-1)^{n+1}}{\lambda_n^3\cosh(\lambda_n L_z/2)}\cos(\lambda_n x)\cosh(\lambda_n z)\right] \tag{26}$$

with $\lambda_n = (2n+1)\pi/L_x$.

Substitution of Eq. (26) into Eq. (6) provides a second relation between the molten layer thickness δ and the melting speed V:

$$\frac{\mu_f V}{\delta^3}\left[L_z L_x^3 - \frac{192 L_x^4}{\pi^5}\sum_{n=0}^{\infty}\frac{\tanh(\lambda_n L_z/2)}{(2n+1)^5}\right] = \rho_s L_x L_z (H - S)g - 2\sigma_f(L_x + L_z) \tag{27}$$

Eqs. (21) and (27) are now cast in dimensionless form using the variables and parameters defined in Table 1:

$$-\frac{Ste_{\text{eff}}}{\rho^*} = 1 - \exp(V^*\delta^* Pr_f) \tag{28}$$

$$V^* = \frac{C_2\delta^{*3}}{C_1} \tag{29}$$

with

$$C_1 = 1 - \frac{192}{L_z^*\pi^5}\sum_{n=0}^{\infty}\frac{\tanh((2n+1)\pi L_z^*/2)}{(2n+1)^5} \quad \text{and}$$

$$C_2 = \rho^*(H^* - S^*)A - \frac{2}{Oh^2}\left(1 + \frac{1}{L_z^*}\right)$$

Note that the effect of the density difference between the solid and liquid phases is taken into account by the dimensionless ratio ρ^*. C_1 is plotted in Fig. 3. Of particular interest is $C_1 \approx 1$ when $L_z^* \gg 1$(one-dimensional limit) and $C_1 \approx L_z^{*2}$ when $L_z^* \ll 1$ [9].

Table 1
Dimensionless variables and parameters

δ^*	δ/L_x
H^*	H/L_x
S^*	S/L_x
L_z^*	L_z/L_x
V^*	VL_x/ν_f
ρ^*	ρ_s/ρ_f
t^*	$\nu_f t/L_x^2$
A	$L_x^3 g/\nu_f^2$

The Prandtl number Pr_f characterizes the substance, the Stefan number Ste_{eff} ,the relative heating intensity and the Ohnesorge number Oh , the relative magnitude of the surface tension. Solution of Eq. (28) and (29) yields

$$\delta^* = \left(\frac{C_1\ln(1 + Ste_{\text{eff}}/\rho^*)}{C_2 Pr_f}\right)^{1/4} \tag{30}$$

$$V^* = \left(\frac{C_2}{C_1 Pr_f^3}\right)^{1/4}\left(\ln\left(1 + \frac{Ste_{\text{eff}}}{\rho^*}\right)\right)^{3/4} \tag{31}$$

Finally, knowing that $dS^*/dt^* = V^*$ and $S^*(t^* = 0) = 0$, the time varying height of the block is obtained:

$$H^* - S^* = \left[(H^* - C_\sigma)^{3/4} - \frac{3}{4}C_{\text{Ste}}t^*\right]^{4/3} + C_\sigma \tag{32}$$

with

$$C_{\text{Ste}} = \left(\frac{\rho^* A\ln^3(1 + Ste_{\text{eff}}/\rho^*)}{C_1 Pr_f^3}\right)^{1/4} \quad \text{and}$$

$$C_\sigma = \frac{2}{\rho^* AOh^2}\left(1 + \frac{1}{L_z^*}\right)$$

The effective Stefan number Ste_{eff} introduced in Eq. (28) takes into account the sub cooling of the PCM. The net effect of sub cooling is to slow down the melting process as some of the heat released by the heated plate is stored as sensible heat in the solid phase of the PCM block. The effective Stefan number is defined as

$$Ste_{\text{eff}} = \frac{C_f\Delta T}{h_{fs} + C_s T_{sc}} \tag{33}$$

which can be rewritten as

$$Ste_{\text{eff}} = \frac{Ste}{1 + Ste_{sc}} \tag{34}$$

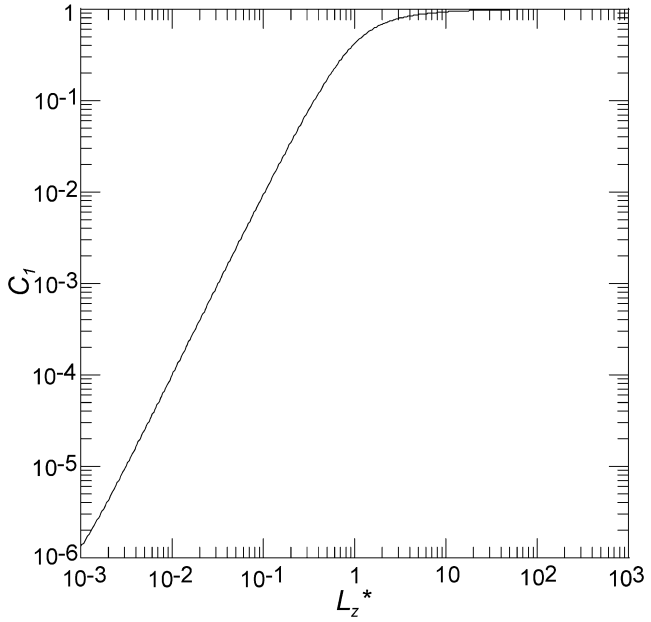

Fig. 3. C_1 versus L_z^*.

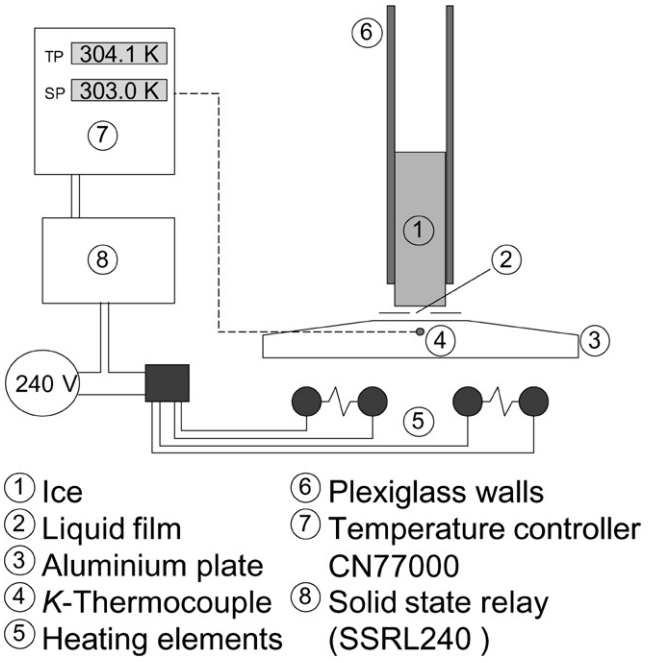

Fig. 4. Schematic of the experimental set-up.

3. Experimental setup

An experimental rig was erected in order to check the validity of the above analytical model. A schematic of the experimental set-up is shown in Fig. 4. A sample of sub cooled ice ($T_{sc} = 22$ K), prepared with tap water, 0.03 m wide, 0.03 m deep and 0.076 m high, held in a rectangular duct made with plexiglass walls, rests on a flat aluminium plate heated by electric resistances. The plate is shaped so as to remove any excess liquid from underneath the sample. A K-type thermocouple, accurate to ± 1 K, is embedded 0.00625 m below the surface of the plate. It is connected to a temperature controller micromega series CN77000. The temperature of the heated plate is controlled using an on/off solid state relay (series SSRL240) from Omega. The time varying height of the melting ice block is measured with a ruler, fixed to the transparent wall of the duct, and a stop watch.

Experiments were conducted for four different plate temperatures ranging from 296 K to 326 K which correspond to Stefan numbers Ste_{eff} of 0.343, 0.497, 0.642 and 0.772 respectively. The resulting dimensionless melting profiles ($(H^* - S^*)$ vs t^*) are depicted in Fig. 5. The error bars represent the area of multiple data measured under identical conditions. As expected, the melting speed increases with the plate temperature and it decreases as the weight (or height) of the PCM block diminishes. Moreover, these experiments have shown that for $(H^* - S^*) < 0.4$, buoyancy forces play a role in contact melting. Towards the end of the melting process, the now lighter ice block floats on a liquid film maintained by surface tension. Consequently, it is expected that the predictions made with the revised model might not fully capture the physics of the melting process for $(H^* - S^*) < 0.4$.

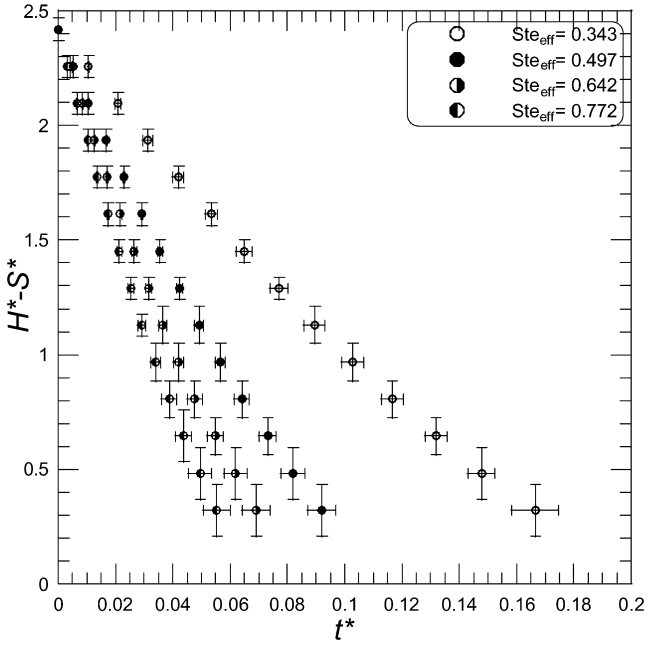

Fig. 5. Experimental results for $H^* - S^*$ versus t^*.

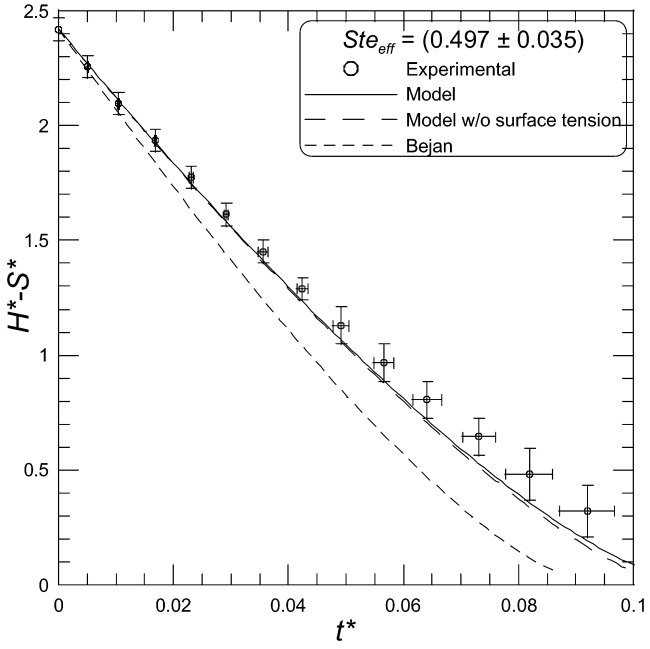

Fig. 6. $H^* - S^*$ versus t^* for $Ste_{\text{eff}} = 0.497$.

4. Results and discussion

Figs. 6 and 7 compare the measured and the predicted melting profiles for $Ste_{\text{eff}} = 0.50$ and $Ste_{\text{eff}} = 0.77$ respectively. In all cases presented here, $L_z^* = 1$ and $C_1 = 0.4217$. Examination of these figures reveals that Bejan's conduction dominated contact melting model overestimates the melting rate for $Ste_{\text{eff}} > 0.1$. The predictions made with the present convection dominated model are, however, in better agreement with the experimental data. It is believed that the slight discrepancy results from the u and w velocity components which are different

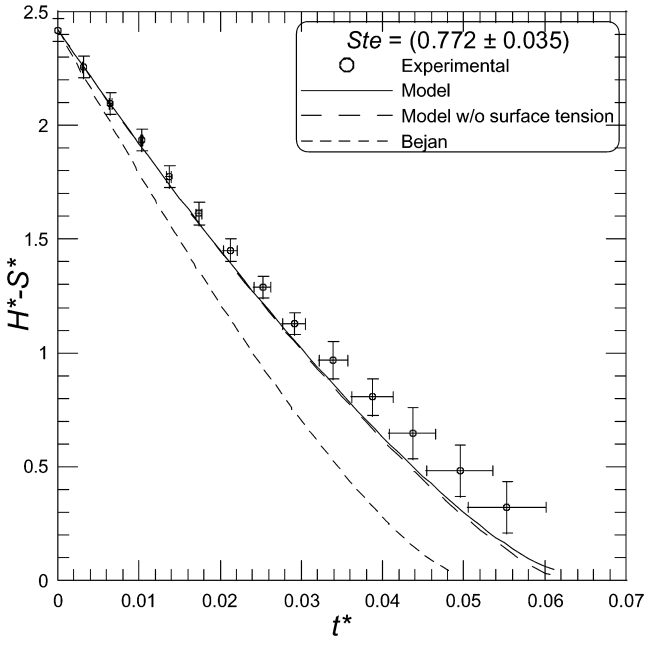

Fig. 7. $H^* - S^*$ versus t^* for $Ste_{\text{eff}} = 0.772$.

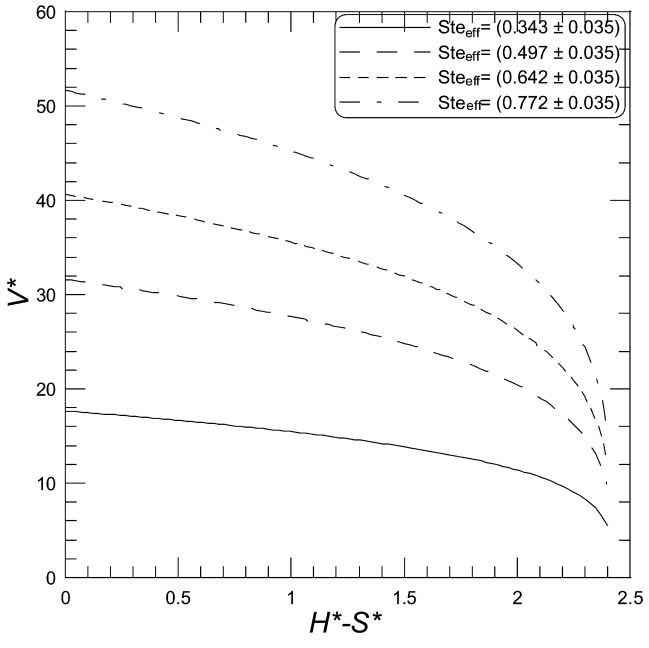

Fig. 9. V^* versus $H^* - S^*$.

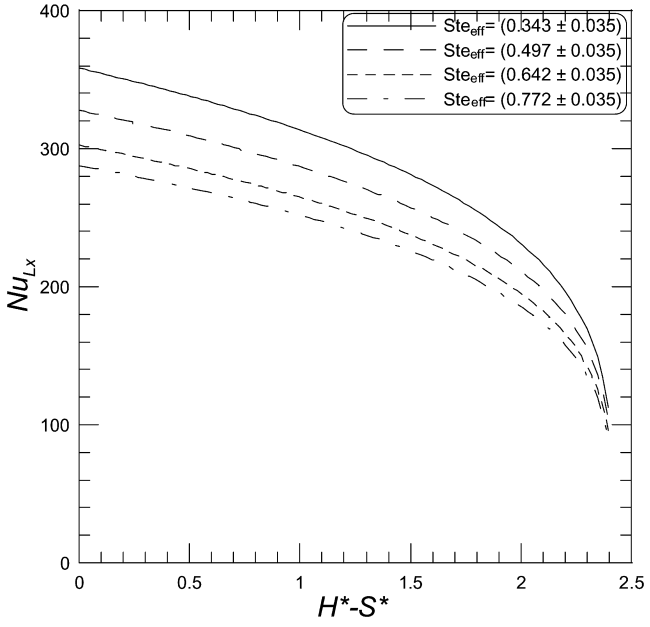

Fig. 8. Nu_{L_x} versus $H^* - S^*$.

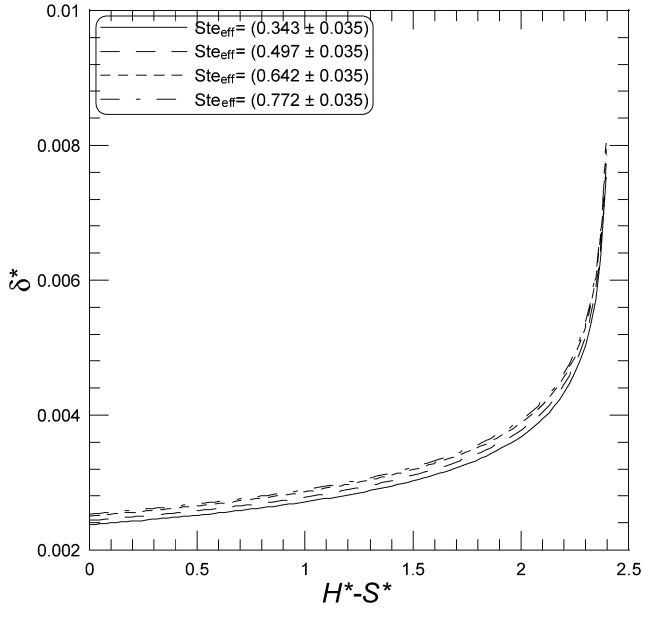

Fig. 10. δ^* versus $H^* - S^*$.

in the model and in the laboratory. Indeed, in the mathematical model, the flow in the melt layer is assumed to behave as a Poiseuille flow, whereas in the laboratory, the flow is perturbed by the imperfections in the experimental setup and on the surface of the heated plate. On the other hand, it is seen that the effect of surface tension cannot be ignored near the end of the melting process, i.e. for $(H^* - S^*) < 0.9$.

The variation of the predicted Nusselt number Nu_{L_x} and of the melting speed V^* at the melting interface in terms of the height $(H^* - S^*)$ are depicted in Figs. 8 and 9 respectively. The Nusselt number is defined as:

$$Nu_{L_x} = \frac{q''}{k_{\text{f}} \Delta T / L_x} = -\frac{\mathrm{d}T/\mathrm{d}y|_{y=\delta}}{\Delta T / L_x} \tag{35}$$

and the melting speed is related to the Nusselt number via the following expression

$$V^* = \frac{Ste_{\text{eff}}}{\rho^* Pr_{\text{f}}} Nu_{L_x} \tag{36}$$

It is seen that as melting proceeds, the decrease in the Nusselt number and in the melting speed is accentuated. This behaviour is due to the increasing thickness of the melt layer δ^* (Fig. 10). Towards the end of the melting process, the thickness of the liquid film augments sharply as the pressure exerted by the melting solid block becomes very small. As a result, the thermal resistance across this layer increases and the Nusselt number and the melting speed drop sharply.

5. Concluding remarks

A study was conducted to examine the role of convection on close contact melting of a high Prandtl number phase change material resting on a heated flat plate. A convection dominated close contact melting model was proposed and its predictions were compared to a conduction dominated model and to experimental data. The main conclusions that can be drawn from this study are:

- Convection plays an important role in the process of close contact melting for $Ste_{\text{eff}} \geqslant 0.1$. Convection reduces the heat flux at the solid–liquid interface thereby slowing down the melting rate. Neglecting convection heat transfer for cases in which $Ste_{\text{eff}} \sim 1$ yields discrepancies of the order of 30% between the predicted and the measured melting rates;
- The effect of inertia forces are negligible at all times for high Prandlt number substances;
- For $(H^* - S^*) < 0.9$, that is near the end of the melting process, surface tension cannot be ignored. Surface tension slows down the process of close contact melting;
- For $(H^* - S^*) < 0.4$, buoyancy starts to play a role in the balance of forces. From this point on, the remaining ice floats on the liquid film and the heat transfer is further diminished.

Acknowledgements

The authors are grateful to the Natural Sciences and Engineering Research council of Canada and to the Fonds Québécois de la Recherche sur la nature et les technologies for their financial support.

References

[1] A. Bejan, Contact melting heat transfer and lubrication, Adv. Heat Transfer 24 (1994) 1–38.
[2] A.J. Fowler, A. Bejan, Contact melting during sliding on ice, Int. J. Heat Mass Transfer 36 (5) (1993) 1171–1179.
[3] J.M. Khodadadi, Y. Zhang, Effects of buoyancy-driven convection on melting within spherical containers, Int. J. Heat Mass Transfer 44 (2001) 1605–1618.
[4] M.K. Moallemi, B.W. Webb, R. Viskanta, An experimental and analytical study of close-contact melting, J. Heat Transfer 108 (1986) 894–899.
[5] I. Sezai, A.A. Mohamad, Natural convection in a rectangular cavity heated from below and cooled from the top as well as the sides, Phys. Fluids 12 (2) (2000) 432–443.
[6] M. Ibrahim, P. Sokolov, T. Kerslake, C. Tolbert, Experimental and computational investigations of phase change thermal energy storage canisters, J. Solar Energy Eng. 122 (2000) 176–182.
[7] H. Hong, A. Saito, Numerical method for direct contact melting in transient process, Int. J. Heat Mass Transfer 36 (1993) 2093–2103.
[8] A. Saito, H. Hong, O. Hirokane, Heat transfer enhancement in the direct contact melting process, Int. J. Heat Mass Transfer 35 (1992) 295–305.
[9] M. Lacroix, Contact melting of a phase change material inside a heated parallelepipedic capsule, Energy Conversion & Management 42 (2001) 35–47.
[10] M. Bareiss, H. Beer, An analytical solution of the heat transfer process during melting of an unfixed solid phase change material inside a horizontal tube, Int. J. Heat Mass Transfer 27 (1984) 739–745.
[11] A. Saito, Y. Utaka, M. Akiyoshi, K. Katayama, On the contact heat transfer with melting (2nd report: analytical study), Bull. JSME 28 (1985) 1703–1709.
[12] S.K. Roy, S. Sengupta, The melting process within spherical enclosures, J. Heat Transfer 109 (1987) 460–462.
[13] T. Hirata, Y. Makino, Y. Kaneko, Analysis of close-contact melting for octadecane and ice inside isothermally heated horizontal rectangular capsule, Int. J. Heat Mass Transfer 34 (1991) 3091–3106.
[14] W.Z. Chen, S.M. Cheng, Z. Luo, W.M. Gu, Analysis of contact melting of phase change materials inside a heated rectangular capsule, Int. J. Energy Res. 19 (1995) 337–345.
[15] A. Bejan, Convection Heat Transfer, second ed., Wiley-Interscience, New York, 1995 (pp. 434–438).
[16] D. Groulx, M. Lacroix, Effects of convection and inertia on close contact melting, Int. J. Thermal Sci. 42 (2003) 1073–1080.
[17] K. Taghavi, Analysis of direct-contact melting under rotation, J. Heat Transfer 112 (1990) 137–143.
[18] H. Yoo, H. Hong, C.J. Kim, Effect of transverse convection and solid–liquid density difference on the steady close-contact melting, Int. J. Heat Fluid Flow 19 (1998) 368–373.